Redox Biology 38 (2021) 101776

Contents lists available at ScienceDirect

Redox Biology

journal homepage: www.elsevier.com/locate/redox

Mono-2-ethylhexyl phthalate drives progression of PINK1-parkin-mediated mitophagy via increasing mitochondrial ROS to exacerbate cytotoxicity

Jian Xu [a,b,1], Liming Wang [c,1], Lihuan Zhang [a], Fang Zheng [a], Fang Wang [a], Jianhang Leng [b], Keyi Wang [b], Paul Héroux [d], Han-Ming Shen [e], Yihua Wu [a,*], Dajing Xia [a,**]

[a] Department of Toxicology of School of Public Health, And Department of Gynecologic Oncology of Women's Hospital, Zhejiang University School of Medicine, Hangzhou, 310058, PR China
[b] Department of Central Laboratory, Affiliated Hangzhou First People's Hospital, Zhejiang University School of Medicine, Hangzhou, 310006, PR China
[c] Hunan Key Laboratory of Medical Epigenomics, Department of Dermatology, Second Xiangya Hospital, Central South University, Changsha, China
[d] Department of Epidemiology, Biostatistics and Occupational Health, McGill University, Canada
[e] Faculty of Health Sciences, University of Macau, Macau SAR, China

ARTICLE INFO

Keywords:
MEHP
Mitochondrial ROS
PINK1-Parkin-mediated mitophagy
Cytotoxicity
Cell death

ABSTRACT

Phthalate ester plasticizers are used to improve the plasticity and strength of plastics. One of the most widely used and studied, di-2-ethylhexyl phthalate (DEHP), has been labeled as an endocrine disruptor. The major and toxic metabolic derivative of DEHP, mono-2-ethylhexyl phthalate (MEHP), is capable of interfering with mitochondrial function, but its mechanism of action on mitophagy remains elusive. Here, we report that MEHP exacerbates cytotoxicity by amplifying the PINK1-Parkin-mediated mitophagy pathway. First, MEHP exacerbated mitochondrial damage induced by low-dose CCCP via increased reactive oxygen species (ROS) production, decreased mitochondrial membrane potential (MMP), and enhanced fragmentation in mitochondria. Second, co-exposure to MEHP and CCCP ("MEHP-CCCP") induced robust mitophagy. Mechanistically, MEHP-CCCP stabilized PINK1, increased the level of phosphorylated ubiquitin (pSer 65-Ub), and led to Parkin mitochondrial translocation and activation. Third, MEHP-CCCP synergistically caused more cell death, while inhibition of mitophagy, either through chemical or gene silencing, reduced cell death. Finally and importantly, co-treatment with N-acetyl cysteine (NAC) completely counteracted the effects of MEHP-CCCP, suggesting that mitochondrial ROS played a vital role in this process. Our results link mitophagy and MEHP cytotoxicity, providing an insight into the potential roles of endocrine disrupting chemicals (EDCs) in human diseases such as Parkinson's disease.

1. Introduction

Endocrine disrupting chemicals (EDCs) are a series of compounds from the external environment that mimic or block endogenous hormones even at low doses [1]. They interfere with natural hormones in many ways, including synthesis, secretion, transport and metabolism, resulting in dysfunction of reproduction [2], immunity [3] as well as the nervous system [4]. Harm from EDCs exposure has gradually aroused attention of academia, the public, and government since the 1990s [5]. Hundreds of environmental chemicals have been confirmed or suspected to have endocrine disrupting effects, and many of them act on estrogen. Environmental estrogen disruptors fall into the following classes [6]: polychlorinated biphenyls (PCBs), alkylphenols (APs), phthalate esters (PAEs), bisphenols (BPs), organochlorine pesticides (OCPs) and herbicides (OCHs), phytoestrogens (PEs), fungal estrogens (FEs), and metals.

Phthalate esters are widely used to improve the plasticity and strength of plastics in many products including toys, medical materials, decorative materials, toiletries and even food packaging [7]. Phthalate esters can be divided into 8 sub-types according to their structures, and among them di-2-ethylhexyl phthalate (DEHP) is the most widely used and studied. DEHP can be slowly released from plastics to the atmosphere, soil, and water over time, causing damage to the environment and organisms [8]. Mono-2-ethylhexyl phthalate (MEHP), one of the primary metabolites of DEHP, is considered to be more toxic than DEHP

* Corresponding author.
** Corresponding author.
E-mail addresses: georgewu@zju.edu.cn (Y. Wu), dxia@zju.edu.cn (D. Xia).
[1] These authors contributed equally to this work.

https://doi.org/10.1016/j.redox.2020.101776
Received 19 June 2020; Received in revised form 20 October 2020; Accepted 27 October 2020
Available online 1 November 2020

[9].

Macroautophagy (hereafter referred to as autophagy) is an evolutionarily conserved catabolic process used to maintain intracellular homeostasis through the degradation of protein aggregates and/or damaged organelles [10–12]. Depending on the nature of the substrates, autophagy can be divided into selective or non-selective autophagy. Selective autophagy targets specific organelles such as mitochondria (mitophagy), ribosomes (ribophagy), endoplasmic reticulum (ER-phagy) and peroxisomes (pexophagy) [13]. Among them, mitophagy is the most well-studied type of selective autophagy. One well-established mitophagy mechanism is the PTEN-induced putative kinase 1 (PINK1)-Parkin-dependent pathway. Once mitochondria are damaged and depolarized, PINK1, a serine/threonine kinase, is stabilized and activated on the outer mitochondrial membrane (OMM) [14]. PINK1 then phosphorylates its key substrates ubiquitin (Ub) and Parkin, leading to Parkin mitochondrial translocation and activation [15]. As an E3 Ub ligase, Parkin ubiquitinates multiple mitochondrial substrates and itself, which in turn recruits further rounds of Parkin onto mitochondria. PINK1, pSer 65-Ub and Parkin form the feedforward mechanism to induce robust mitophagy, and quickly remove the damaged mitochondria [16,17].

Since mitochondria are the main venues of oxidative phosphorylation and adenosine triphosphate (ATP) production in eukaryotic cells, defective mitophagy leads to accumulation of damaged mitochondria and increased ROS production. On the other hand, many extracellular stimuli are capable of promoting the production of mitochondrial ROS, onset of mitophagy and activation of cell death [18]. However, the causative role of ROS in the process of mitophagy and cell death remains largely elusive. Joselin et al. reported that ROS elimination inhibited Parkin mitochondrial translocation and mitophagy in mouse embryonic fibroblasts [19], whereas Xiao et al. showed that pro-oxidants such as H_2O_2 did not induce mitophagy themselves, but functioned as mitophagy promoters when mitochondria were damaged by agents such as CCCP [20]. Mitophagy is usually considered as a cell survival mechanism as it eliminates damaged mitochondria [18]. However, it has also been reported that abnormal or excessive mitophagy contributes to cell death [21–23].

MEHP has been reported to reduce mitochondrial membrane potential (MMP) [24,25] and inhibit the production of ATP [26]. DEHP and MEHP are also shown to induce mitochondrial apoptosis [27,28]. However, whether MEHP regulates mitophagy, and the contribution of mitophagy to its toxicity have not been examined. In this study, we find that upon mitochondrial damage, MEHP exposure dramatically amplifies this damage, and promotes mitophagy. More importantly, mitophagy promoted by MEHP acts as a cell death mechanism to increase the cytotoxicity of MEHP. Thus, this novel regulatory function of MEHP in mitophagy offers a new insight into the disrupting effects of EDCs on human diseases such as cancer, heart failure, and neurodegenerative diseases.

2. Materials and methods

2.1. Reagents and antibodies

Our experiments used the following reagents: Mono-2-ethylhexyl phthalate (MEHP, Sigma 796,832), Di-2-ethylhexyl phthalate (DEHP, Sigma 80,030), Carbonyl cyanide 3-chlorophenylhydrazone (CCCP, Sigma C2759), N-Acetyl Cysteine (NAC, Merck), Z-VAD (OMe)-FMK (Santa Cruz, CAS 187389-52-2), Bafilomycin A1 (BafA1, Sigma B1793), MitoSOX™ (Invitrogen, M36008), MitoProbe™ $DiIC_1(5)$ Assay Kit (Invitrogen, M34151), Tetramethylrhodamine, Ethyl Ester, Perchlorate (TMRE) (Abcam, ab113852), Propidium iodide (PI, Sigma P4170), Annexin V FITC (Invitrogen, V13242). We used the following antibodies: anti-phospho-DRP1 (Ser616) antibody (CST, 3455), anti-phospho-DRP1 (Ser637) antibody (CST, 4867), anti-DRP1 (D6C7) antibody (CST, 8570), anti-HSP60 (D6F1) antibody (CST, 12,165), anti-Parkin antibody (Santa Cruz, SC32282), anti-PINK1 (D8G3) antibody (CST, 6946), anti-Tim23 (H-8) antibody (Santa Cruz, SC514463), anti-Tom20 (FL-145) antibody (Santa Cruz, SC11415), anti-COXIV (3E11) antibody (CST, 4850), anti-Mitofusin-1 (D6E2S) antibody (CST, 14,739), anti-Mitofusin-2 (D1E9) antibody (CST, 11,925), anti-VDAC antibody (CST, 4866), anti-microtubule-associated protein 1 light chain 3/LC3 antibody (Sigma, L7543), anti-p62 antibody (Sigma, SAB1406748), anti-phospho-ubiquitin antibody (Merck Millipore, ABS1513-I), anti-ubiquitin (P4D1) antibody (Santa Cruz, SC8017), anti-β-actin antibody (Sigma, A5441).

2.2. Cell culture

Human neuroblastoma SH-SY5Y cells and HeLa cells were obtained from the American Type Culture Collection (ATCC). HeLa cells stably expressing YFP-Parkin were kindly provided by Dr. Richard Youle (National Institutes of Health, USA). All cell lines were maintained in Dulbecco's modified Eagle's medium (DMEM, Sigma, D1152) containing 10% fetal bovine serum (HyClone, SV30160.03) and 1% penicillin/streptomycin (Invitrogen) in a 5% CO_2 atmosphere at 37 °C.

2.3. Measurement of mitochondrial ROS production

Cells were cultured in a 12-well plate and treated as indicated. To detect mitochondrial ROS, cells were labeled with MitoSOX™ Red superoxide indicator (Invitrogen, M36008) with a final concentration of 2.5 μM for 30 min. The intensity of red fluorescence was observed and photographed under a fluorescence microscope (Carl Zeiss Axio Observer A1). Cells were then digested by 0.25% trypsin, rinsed with ice-cold phosphate buffer saline (PBS) and finally subjected to flow cytometry (BD FACSCanto II) to quantitatively determine the fluorescence intensity.

2.4. Measurement of mitochondrial membrane potential

Cells were treated as indicated in the figure legends. (I) After treatment, cell pellets were collected and resuspended in MitoProbe™ $DiIC_1(5)$ Assay Kit (Invitrogen, M34151) with a final concentration of 25 nM. After incubation at 37 °C, 5% CO_2 for 15 min, cells were centrifuged and resuspended in 500 μL ice-cold PBS and subsequently analyzed on a flow cytometer with 633 nm excitation to determine the fluorescence intensity. (II) After treatment, cell pellets were stained with Tetramethylrhodamine, Ethyl Ester, Perchlorate (TMRE) (Abcam, ab113852) with a final concentration of 200 nM for 20 min. Cells were collected and resuspended in 500 μL ice-cold PBS and subsequently analyzed on a flow cytometer to determine the fluorescence intensity.

2.5. Immunoblotting

After all the designated treatments, cells were rinsed with ice-cold PBS and lysed in Laemmli buffer (62.5 mM Tris-HCl, pH 6.8, 20% glycerol, 2% SDS, 2 mM dithiothreitol (DTT), phosphatase inhibitor and proteinase inhibitor cocktail). Cell lysates were collected and boiled for 5 min at 100 °C. An equal amount of protein was analyzed using high resolution SDS-PAGE gel and transferred onto nitrocellulose (NC) filter membrane. Membranes were blocked in 5% defatted milk for 1 h and subsequently subjected to first and second antibodies. Results were visualized by a Kodak Image Station 4000R (Kodak) combined with the enhanced chemiluminescence method (Thermo Scientific, 34,076). For quantification of the mitochondrial markers, densitometry analysis of corresponding bands was performed using ImageJ software, and the fold change was calculated by comparing the treated groups with the respective control dimethyl sulfoxide (DMSO) groups.

2.6. Immunofluorescence staining

Cells were seeded on a cover glass and treated as indicated. After rinsing with PBS, the cells were fixed with 4% paraformaldehyde (PFA) in PBS for 10 min and then permeabilized with 1% Triton X-100 in PBS for another 10 min. After blocking in 5% BSA for 30 min, cells were incubated in the designated first antibody overnight. On the second day, cells were incubated in the second antibody for 1 h, followed by DAPI (1:10,000) staining for 10 min. The cells were finally examined under a fluorescence microscope and random fields were photographed.

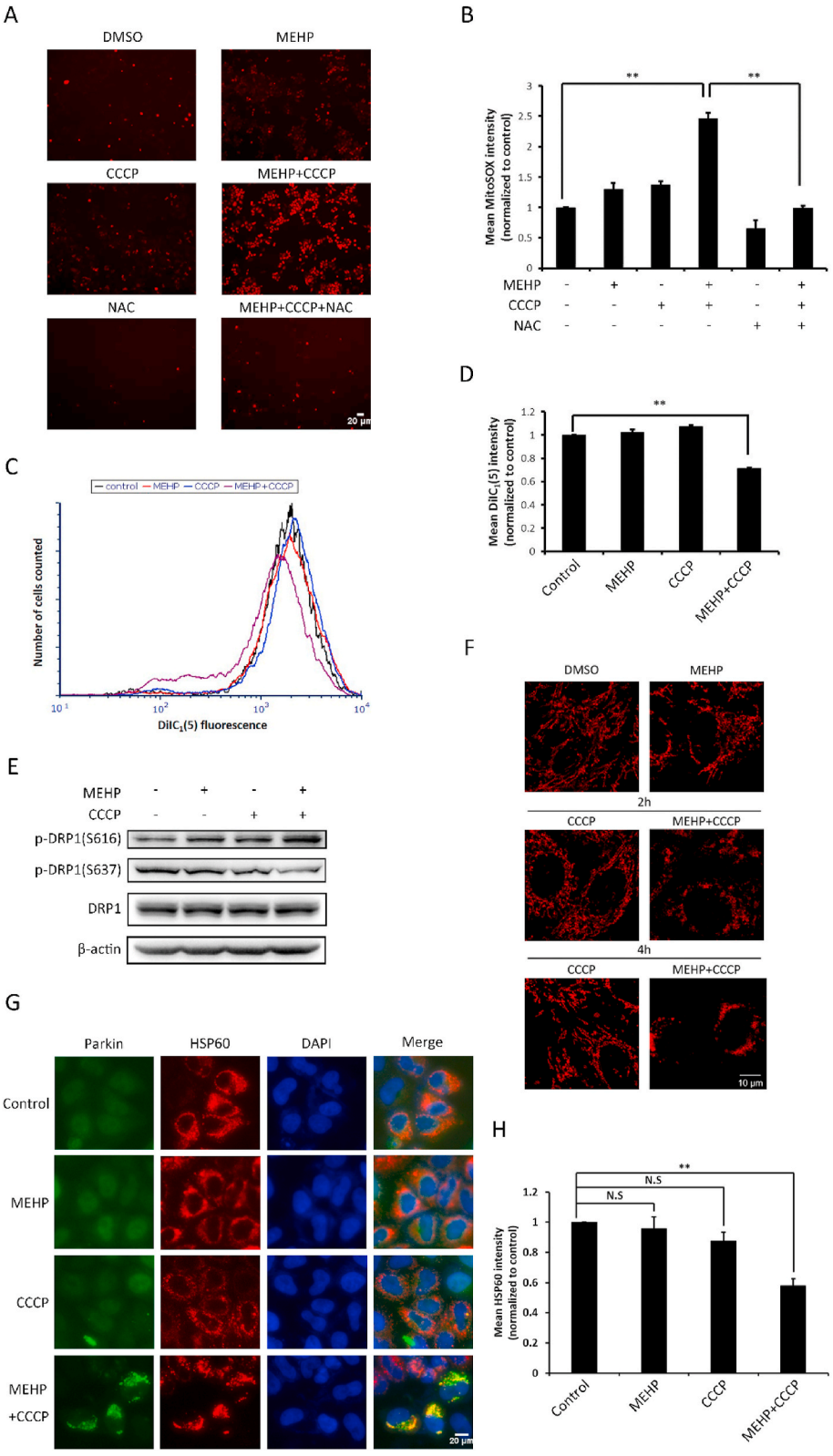

Fig. 1. MEHP-CCCP induces mitochondrial damage. (A) HeLa cells stably expressing YFP-Parkin were exposed to MEHP (200 μM, 24 h) or CCCP (2.5 μM, 2 h) respectively, or pre-exposed to MEHP (200 μM) for 24 h, followed by CCCP (2.5 μM) for 2 h in the presence or absence of NAC (5 mM). After incubation with MitoSOX™ (2.5 μM) for 30 min, cells were examined and representative cells were photographed using a fluorescence microscope. Scale bar, 20 μm. **(B)** HeLa-YFP-Parkin cells were treated as in (A). Cell pellets were subsequently collected and subjected to flow cytometry to detect the fluorescence intensity. Data (means ± SD) were representative of three independent experiments (**, $P < 0.01$, Student's *t*-test). **(C)** HeLa-YFP-Parkin cells were exposed to MEHP (200 μM, 24 h) or CCCP (2.5 μM, 6 h) respectively, or pre-exposed to MEHP (200 μM) for 24 h, followed by CCCP (2.5 μM) for 6 h. Cells were collected and incubated with $DiIC_1(5)$ (25 nM) for 15 min, the fluorescence intensity was analyzed by flow cytometry. **(D)** Statistical analysis of the fluorescence intensity of HeLa-YFP-Parkin cells as treated in (C). Data (means ± SD) were representative of three independent experiments (**, $P < 0.01$, Student's *t*-test). **(E)** HeLa-YFP-Parkin cells were treated as in (A), and cell lysate was harvested for Western blot detection of DRP1 phosphorylation status. **(F)** HeLa-YFP-Parkin cells were either exposed to MEHP (200 μM, 24 h) or CCCP (2.5 μM, 2 h) respectively, or pre-exposed to MEHP (200 μM) for 24 h, followed by CCCP (2.5 μM) for 2 h or 4 h. Cells were subjected to immunostaining of Tom20 (red) and observed by FV3000 confocal laser scanning microscope. Scale bar, 10 μm. **(G)** Cells stably expressing YFP-Parkin (green) were treated as in (A) and subjected to immunostaining of HSP60 (red). DNA was stained by DAPI (blue). Cells were examined and photographed using a fluorescence microscope. Scale bar, 20 μm. **(H)** Statistical analysis of the fluorescence intensity of HSP60 as treated in (G). Data (means ± SD) were representative of three independent experiments (**, $P < 0.01$; N·S, $P > 0.05$; Student's *t*-test). (For interpretation of the references to colour in this figure legend, the reader is referred to the Web version of this article.)

2.7. Small interfering RNA (siRNA) and transient transfection

The PINK1 siRNA (target sequences: CCAUCAAGAUGAUGUGGAATT; AATTCCACAUCAUCUUGAUGG) and scramble siRNA were transfected into cells by Powerfect™ siRNA Transfection Reagent (SignaGen) according to the manufacturer's instructions when cells were grown to 30%–40% confluency.

2.8. Detection of cell death

The following methods were applied to detect cell death qualitatively and quantitatively: (I) Morphological changes under a phase-contrast microscope. (II) Propidium iodide (PI) live cell exclusion assay coupled with flow cytometry for the detection of cell viability. (III) PI/Annexin V or PI/DiIC$_1$(5) double staining combined with flow cytometry for the evaluation of apoptosis. For (II) and (III), after treatments, cells were harvested by 0.25% trypsin and cell pellets were obtained by centrifugation. Cells were then incubated with PI (5 μg/mL) or PI/Annexin V or PI/DiIC$_1$(5) (1 μg/mL, 50 nM) for 5 min and subjected to flow cytometry for analysis of fluorescence intensity.

2.9. Statistical analysis

Statistical data are presented as means ± SD from 3 independent experiments, and analyzed using Student's *t*-test or one-way ANOVA to determine statistically significant differences at $P < 0.05$.

3. Results

3.1. MEHP-CCCP causes mitochondrial damage and dysfunction

To explore the possible role of MEHP in the regulation of mitophagy, we first performed several screening experiments to determine the appropriate working concentrations for MEHP and CCCP. As shown in Fig. S1A to S1F, we found that lower concentration of CCCP (2.5 μM) or different concentrations of single MEHP exposure had no effects on MMP (TMRE probe) and Parkin mitochondrial translocation, while higher concentration of MEHP (400 μM) exposure alone is too toxic for cells. Thus, we selected 200 μM for MEHP and 2.5 μM for CCCP, respectively, for most of the subsequent experiments. Next, we treated HeLa cells stably expressing YFP-Parkin with MEHP for 24 h, and then measured mitochondrial ROS production using the MitoSOX™ probe. As shown in Fig. 1A, modest red fluorescence was observed, suggesting that MEHP did not increase the level of mitochondrial ROS. Similarly, CCCP treatment for 2 h only induced slight red fluorescence. However, to our surprise, a significant increase of red fluorescence was observed if exposure to MEHP for 24 h was followed by CCCP exposure for another 2 h ("MEHP-CCCP"). Moreover, N-Acetyl Cysteine (NAC), a well-known cell penetrating antioxidant, unequivocally reduced ROS production (Fig. 1A). To further confirm our finding, we employed flow cytometry to measure the fluorescence intensity with the MitoSOX™ probe. We consistently found that MEHP-CCCP increased mitochondrial ROS production by approximately 1.9 and 1.8 times compared to separate MEHP or CCCP treatment (Fig. 1B). Then, we used another classic MMP detection kit (DiIC$_1$(5) probe) to test the effect of MEHP on MMP, which is essential to maintain the physiological functions of mitochondria. Consistently, we found that MEHP-CCCP significantly reduced MMP, while individual treatments had no obvious effects (Fig. 1C and D).

It is well known that mitochondria are dynamic organelles, and constantly undergo fission and fusion events. The reduction of MMP probably leads to imbalance between fission and fusion [29]. The DRP1 protein, one member of the dynamin family of large GTPases, is a key controller of mitochondrial fission [30]. The post-translational modifications of DRP1, such as phosphorylation, SUMOylation and ubiquitination, can alter its activity, and consequently affect mitochondrial fission rates [31]. For example, DRP1 can be phosphorylated at different sites, some of which, such as phosphorylation of DRP1 at Ser637 (pSer637-DRP1) by protein kinase A (PKA), can inhibit fission [32], whereas phosphorylation at Ser616 (pSer616-DRP1) by Ca^{2+}/calmodulin-dependent kinase II (CaMKII), can promote fission [33]. Thus, we wondered whether MEHP could alter the phosphorylation of DRP1. Indeed, our Western blot data clearly showed that MEHP-CCCP significantly increased pSer616-DRP1, but decreased pSer637-DRP1 (Fig. 1E), suggesting that this treatment enhanced mitochondrial fission. Next, we used high-resolution microscopy to observe the changes of mitochondrial morphology, and found that MEHP-CCCP obviously caused mitochondrial fragmentation at different time points (Fig. 1F). We also stained mitochondria with anti-HSP60 antibody, and found that MEHP-CCCP caused mitochondrial aggregation and fragmentation (Fig. 1G). Interestingly, we observed a significant decrease in the intensity of HSP60, indicating the elimination of mitochondria following toxicants exposure (Fig. 1G and H). Collectively, our data showed that MEHP-CCCP caused mitochondrial dysfunction.

3.2. MEHP-CCCP induces mitophagy

Mitophagy is a selective form of autophagy triggered by mitochondrial damage, aiming at elimination of dysfunctional mitochondria [14,15,17]. To evaluate the possible effect of MEHP-CCCP on mitophagy, we examined changes of multiple mitochondrial proteins, including OMM proteins (Tom20, VDAC1, MFN1 and MFN2) and inner mitochondrial membrane (IMM) proteins (Tim23 and COXIV). As shown in Fig. 2A and B, MEHP-CCCP significantly induced the degradation of mitochondrial proteins in SH-SY5Y cells, which expressed endogenous Parkin. Similar results were obtained in HeLa-YFP-Parkin cells, but not in HeLa cells without Parkin expression (Fig. 2C–F), suggesting that Parkin is probably essential in MEHP-CCCP-induced mitophagy. As discussed above, MEHP is the hydrolysate of DEHP [9], however, DEHP induced much lower level of mitophagy (Fig. 2G and H), indicating that MEHP is an activated toxic metabolite of DEHP. We also attempted to study the regulatory effects of MEHP-CCCP on general autophagy, and found that co-exposure had little effect on general autophagy, as evidenced by the absence of changes in LC3 lipidation (LC3-II) and p62 degradation (Fig. S2A and S2B). In addition, we performed time-course studies (0, 2, 4 h) to check autophagic flux in the presence or absence of lysosomal inhibitor Bafilomycin A1 (BafA1). Consistent with our above findings, MEHP-CCCP failed to affect general autophagy (Fig. S2C to S2F).

Parkin plays a key role in the mitophagic process. Mitochondrial depolarization leads to the recruitment of Parkin from cytosol to mitochondria, and activation upon phosphorylation by PINK1 via a well-established feedforward mechanism [14,15,17]. We wondered whether MEHP could have effects on Parkin. Indeed, we found that MEHP effectively promoted Parkin translocation to mitochondria in cells treated with CCCP (Fig. 3A and B and). Moreover, Parkin was auto-ubiquitinated after MEHP-CCCP treatment, but not by MEHP or CCCP exposure alone (Fig. 3C), suggesting the activation of Parkin. Consistently, we also found that endogenous Parkin in SH-SY5Y cells was degraded following ubiquitination (Fig. 3D).

As we had observed the changes in Parkin distribution and activity earlier, we investigated whether MEHP could act upstream of Parkin, such as on PINK1. Indeed, MEHP-CCCP caused accumulation of full length-PINK1 (Fig. 4A andB and). It is well-known that PINK1 is the serine/threonine kinase which phosphorylates Ub [34–37] and Parkin [38,39], leading to the onset of mitophagy. As shown in Fig. 4C, MEHP-CCCP obviously increased the phosphorylation level of Ub (pSer 65-Ub). In order to explore the role of PINK1 in Parkin activation, we introduced the specific PINK1 siRNA to knock down PINK1, and found that this efficiently prevented Ub phosphorylation (Fig. 4D), Parkin mitochondrial translocation (Fig. 4E), as well as Parkin auto-ubiquitination (Fig. 4F), outlining the central role of PINK1 in this process. In addition, knockdown of PINK1 blocked the degradation of mitochondrial proteins (Fig. 4G), demonstrating that

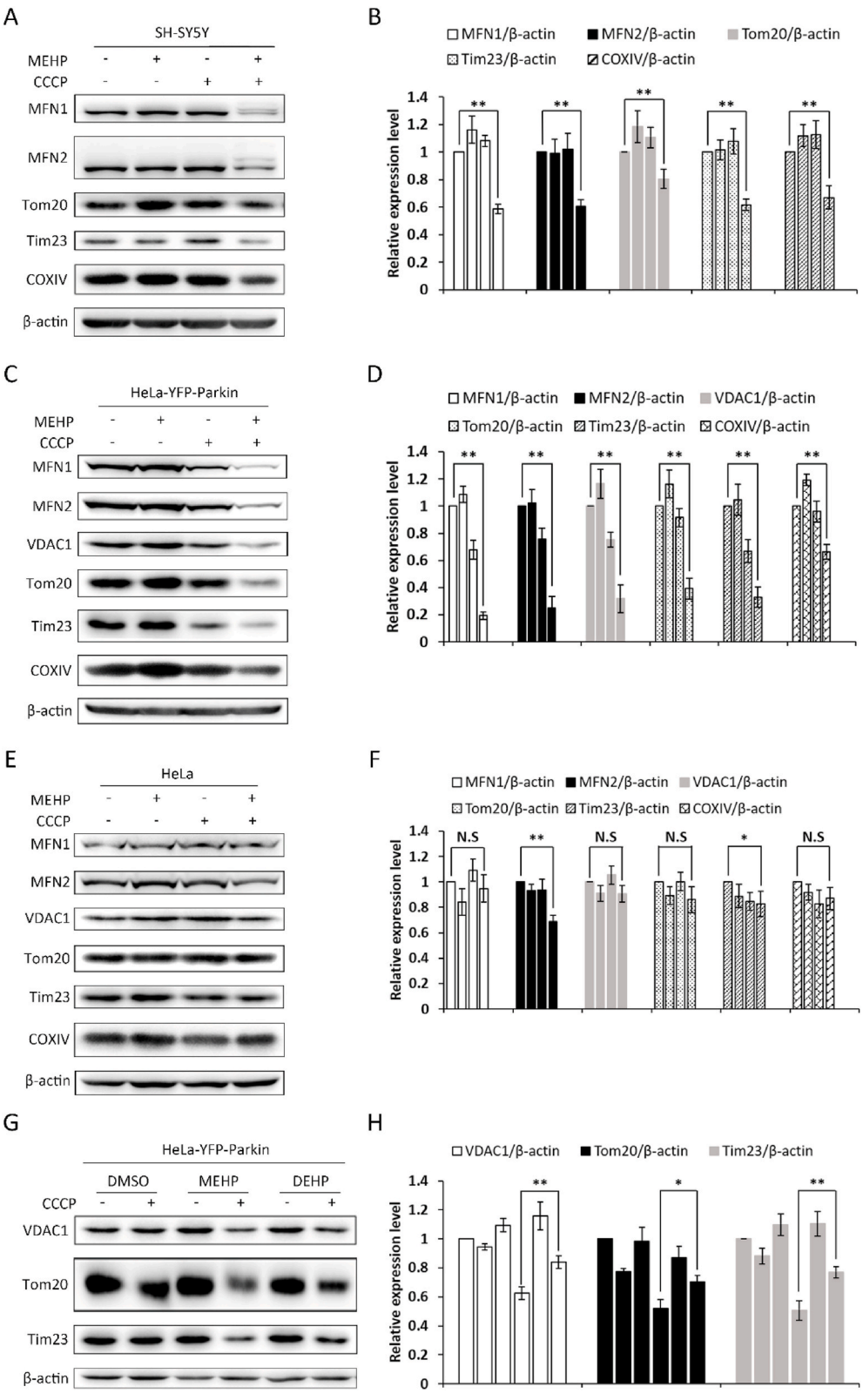

Fig. 2. MEHP-CCCP induces mitophagy. **(A)** SH-SY5Y cells were incubated with MEHP (200 μM) for 24 h or CCCP (5 μM) for 8 h respectively, or pre-incubated with MEHP (200 μM) for 24 h and then incubated with CCCP (5 μM) for 8 h. Western blot was performed to detect proteins expression. **(B)** Proteins expression from (A) was evaluated by ImageJ, means ± SD from 3 independent experiments were presented (**, $P < 0.01$; Student's *t*-test). **(C)** HeLa-YFP-Parkin cells were exposed to MEHP (200 μM, 24 h) or CCCP (2.5 μM, 8 h) respectively, or pre-exposed to MEHP (200 μM) for 24 h, followed by CCCP (2.5 μM) for 8 h. Mitochondrial proteins were evaluated by Western blot. **(D)** Proteins expression from (C) was evaluated by ImageJ, means ± SD from 3 independent experiments were presented (**, $P < 0.01$; Student's *t*-test). **(E)** HeLa cells were treated as in (C). Cell lysate was collected and mitochondrial proteins were detected by Western blot. **(F)** Proteins expression from (E) was evaluated by ImageJ, means ± SD from 3 independent experiments were presented (*, $P < 0.05$; **, $P < 0.01$; N·S, $P > 0.05$; Student's *t*-test). **(G)** HeLa-YFP-Parkin cells were exposed to MEHP (200 μM, 4 h) or CCCP (2.5 μM, 4 h) respectively, or pre-exposed to MEHP (200 μM) for 4 h, followed by CCCP (2.5 μM) for 4 h. Cells were treated with DEHP (200 μM) the same as above, and then harvested and subjected to Western blot for the evaluation of mitochondrial proteins. **(H)** Proteins expression from (G) was evaluated by ImageJ, means ± SD from 3 independent experiments were presented (*, $P < 0.05$; **, $P < 0.01$; Student's *t*-test). MEHP promotes Parkin translocation to damaged mitochondria.

MEHP-CCCP-induced mitophagy was dependent on the expression of PINK1 and Parkin.

3.3. Mitophagy promotes MEHP-CCCP-induced cell death

We then investigated the association between mitophagy and cytotoxicity induced by MEHP-CCCP. As shown from cell morphology in Fig. 5A, MEHP-CCCP significantly increased cell death compared to the individual agents. Quantitative data of cell death by propidium iodide (PI) staining combined with flow cytometry further confirmed this result (Fig. 5B). We also co-treated the cells with Z-Val-Ala-Asp(OMe)-fluoromethylketone (zVAD), an irreversible and cell permeable broad-

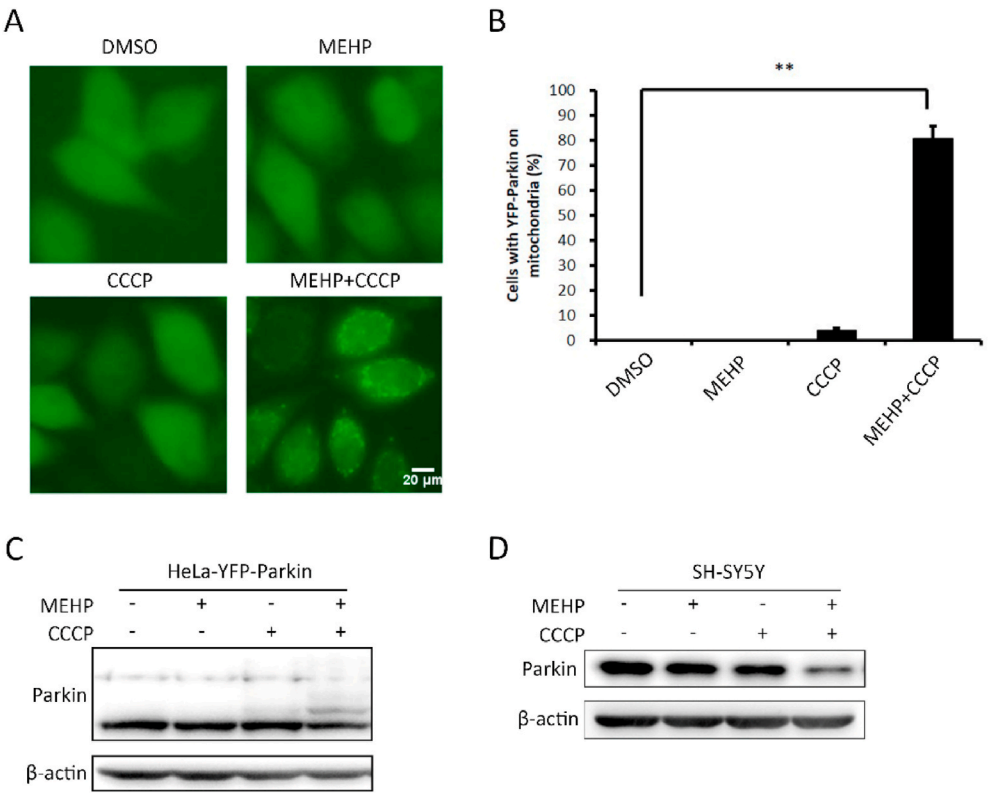

Fig. 3. MEHP promotes Parkin translocation to damaged mitochondria. (A) HeLa-YFP-Parkin cells were either exposed to MEHP (200 μM) for 24 h or CCCP (2.5 μM) for 2 h, or the cells were pre-exposed to MEHP for 24 h, followed by CCCP exposure for 2 h. The localization of YFP-Parkin was observed under a fluorescence microscope. Scale bar, 20 μm. **(B)** The percentage of cells with YFP-Parkin in mitochondria was quantified by ImageJ, means ± SD were presented of three independent experiments (**, $P < 0.01$, Student's *t*-test). **(C)** HeLa-YFP-Parkin cells were treated as in (A), cells were collected and lysed to detect Parkin expression by Western blot. **(D)** SH-SY5Y cells were exposed to MEHP (200 μM, 24 h) or CCCP (5 μM, 8 h) respectively, or pre-exposed to MEHP (200 μM) for 24 h, followed by CCCP (5 μM) for 8 h. Protein level of Parkin was evaluated by Western blot. MEHP-CCCP induces mitophagy in a PINK1-Parkin-dependent manner. (For interpretation of the references to colour in this figure legend, the reader is referred to the Web version of this article.)

spectrum caspase inhibitor, and found that zVAD could not abolish cell death caused by MEHP-CCCP (Fig. 5A and B). $DiIC_1(5)$/PI double staining was then applied to detect the percentage of different types of cell death. As shown in Fig. 5C and D, MEHP-CCCP induced 19.9% of apoptosis and 35.1% of other types of cell death.

To investigate the role of mitophagy in MEHP-CCCP-induced cell death, we repeated the cell death experiments in SH-SY5Y cells with endogenous Parkin expression, and found the same results as Fig. 5A and B (Fig. S3A and S3B). Notably, in normal HeLa cells without Parkin expression, MEHP-CCCP induced much less cell death (Fig. S3C and S3D), suggesting that Parkin is critical in MEHP-CCCP-induced cell death. We then knocked down PINK1 to inhibit mitophagy, and found that cell death was mitigated after PINK1 knockdown (Fig. 5E–G). Moreover, we used the chemical inhibitor BafA1 to inhibit lysosomal degradation, and found that BafA1 co-treatment also decreased cell death induced by MEHP-CCCP, further confirming the pro-death function of mitophagy (Fig. 5H–J).

We had found an increased production of mitochondrial ROS induced by MEHP-CCCP in Fig. 1A and B and . We were then interested to clarify the role of mitochondrial ROS in MEHP-CCCP-induced mitophagy and cell viability. To do this, we first confirmed that NAC indeed neutralized the ROS after 2 h, 8 h or 24 h' treatment (Fig. 1A and B , Fig. S4A and S4B). We then co-treated the cells with NAC, and found that Parkin mitochondrial translocation was dramatically reversed (Fig. 6A). Moreover, the Western blot data showed that full length-PINK1 accumulation, Parkin auto-ubiquitination, as well as mitochondrial proteins degradation were all reversed by NAC co-treatment (Fig. 6B and C), indicating that mitochondrial ROS mediated MEHP-CCCP-induced mitophagy. We further found that NAC co-treatment totally abolished cell death caused by MEHP-CCCP (Fig. 6D–F). All these data strongly suggested that the generation of mitochondrial ROS was the main cause of cytotoxicity induced by MEHP-CCCP.

4. Discussion

The endocrine disrupting effects of EDCs have recently caught substantial attention from the public with increasing awareness to environmental problems. The plasticizer DEHP is known to be an important environmental endocrine disruptor. Once in the body, DEHP is readily hydrolyzed into several primary metabolites, among which MEHP is considered as the main toxicant [9,40]. DEHP and MEHP have been demonstrated to possess reproductive toxicity and neurotoxicity, but the toxic mechanisms are still unclear. It has been reported that MEHP can disturb mitochondrial functions, including inhibition of ATP production [26], reduction of MMP [24,25], and activation of the mitochondria-dependent apoptotic pathways [27,28]. MEHP is also shown to induce ROS-dependent autophagic cell death in human vascular endothelial cells [41]. However, whether MEHP can disturb mitophagy remains largely unknown.

In order to elucidate the role of MEHP in the regulation of mitophagy, and the possible effects of mitophagy on MEHP toxicity, we selected a physiologically relevant cell line human neuroblastoma SH-SY5Y cells with endogenous expression of Parkin, and a classic cell line HeLa cells with exogenous expression of YFP-Parkin as cell models. We first evaluated the effect of MEHP on mitochondrial function. Interestingly, neither MEHP (200 μM) nor CCCP (2.5 μM) exposure alone induced significant mitochondrial damage, whereas the combined exposure (MEHP-CCCP) was sufficient to cause mitochondrial dysfunction, as evidenced by increased mitochondrial ROS production, decreased MMP, up-regulated phosphorylation of mitochondrial fission factor DRP1 (S616), down-regulated phosphorylation of DRP1 (S637) as well as excessive mitochondrial fragmentation (Fig. 1).

Mitophagy selectively degrades damaged mitochondria and has a relatively independent mechanism from bulk autophagy. Mitochondrial damage induced by MEHP-CCCP prompted us to study their effects on mitophagy, and the underlying mechanisms. We found that MEHP-CCCP significantly activated mitophagic response, leading to the degradation of various mitochondrial proteins (Fig. 2). In recent years, PINK1-

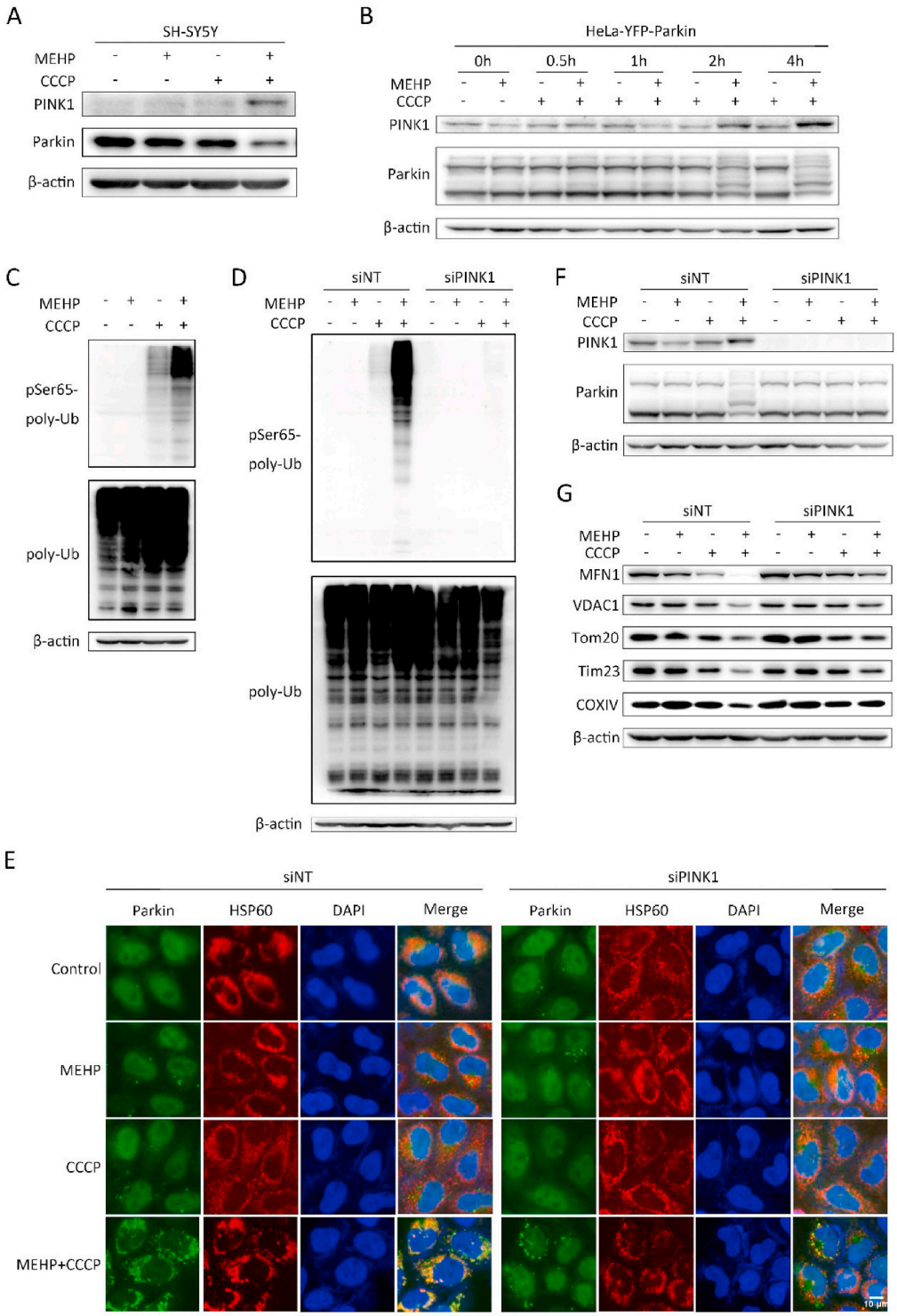

Fig. 4. MEHP-CCCP induces mitophagy in a PINK1-Parkin dependent pathway. (A) SH-SY5Y cells were incubated in MEHP (200 μM, 24 h) or CCCP (5 μM, 8 h) respectively, or pre-incubated in MEHP (200 μM) for 24 h, followed by CCCP (5 μM) for 8 h. PINK1 and Parkin levels were detected by Western blot. **(B)** HeLa-YFP-Parkin cells were exposed to MEHP (200 μM) for 24 h or CCCP (2.5 μM) for 0.5, 1, 2, 4 h respectively, or pre-exposed to MEHP (200 μM) for 24 h, followed by CCCP (2.5 μM) exposure for the indicated time periods. Cell lysate was collected and subjected to Western blot to detect PINK1 and Parkin levels. β-actin was used as a loading control. **(C)** HeLa-YFP-Parkin cells were exposed to MEHP (200 μM) for 24 h or CCCP (2.5 μM) for 2 h respectively, or pre-exposed to MEHP (200 μM) for 24 h, followed by CCCP (2.5 μM) for 2 h. The phosphorylation of ubiquitin (Ser65) was analyzed by Western blot. **(D)** HeLa-YFP-Parkin cells were firstly transfected with a non-targeting siRNA or PINK1 specific siRNA. 48 h after transfection, cells were treated as in (C), Western blot was performed to evaluate the phosphorylation status of ubiquitin (Ser65). **(E)** HeLa-YFP-Parkin cells were treated as in (D). After permeabilization, mitochondria were labeled by HSP60 antibody (1:100) and DNA by DAPI (1:10,000). Cells were observed under a fluorescence microscope. Scale bar, 10 μm. **(F)** Cells were treated as in (D), cell lysate was collected to evaluate the protein levels of PINK1 and Parkin. **(G)** PINK1 was knocked down by siRNA in HeLa-YFP-Parkin cells as in (D). 48 h later, cells were incubated with MEHP (200 μM, 24 h) or CCCP (2.5 μM, 8 h) respectively, or pre-incubated with MEHP (200 μM) for 24 h, followed by CCCP (2.5 μM) for 8 h. Western blot was performed to detect the expression of mitochondrial proteins. (For interpretation of the references to colour in this figure legend, the reader is referred to the Web version of this article.)

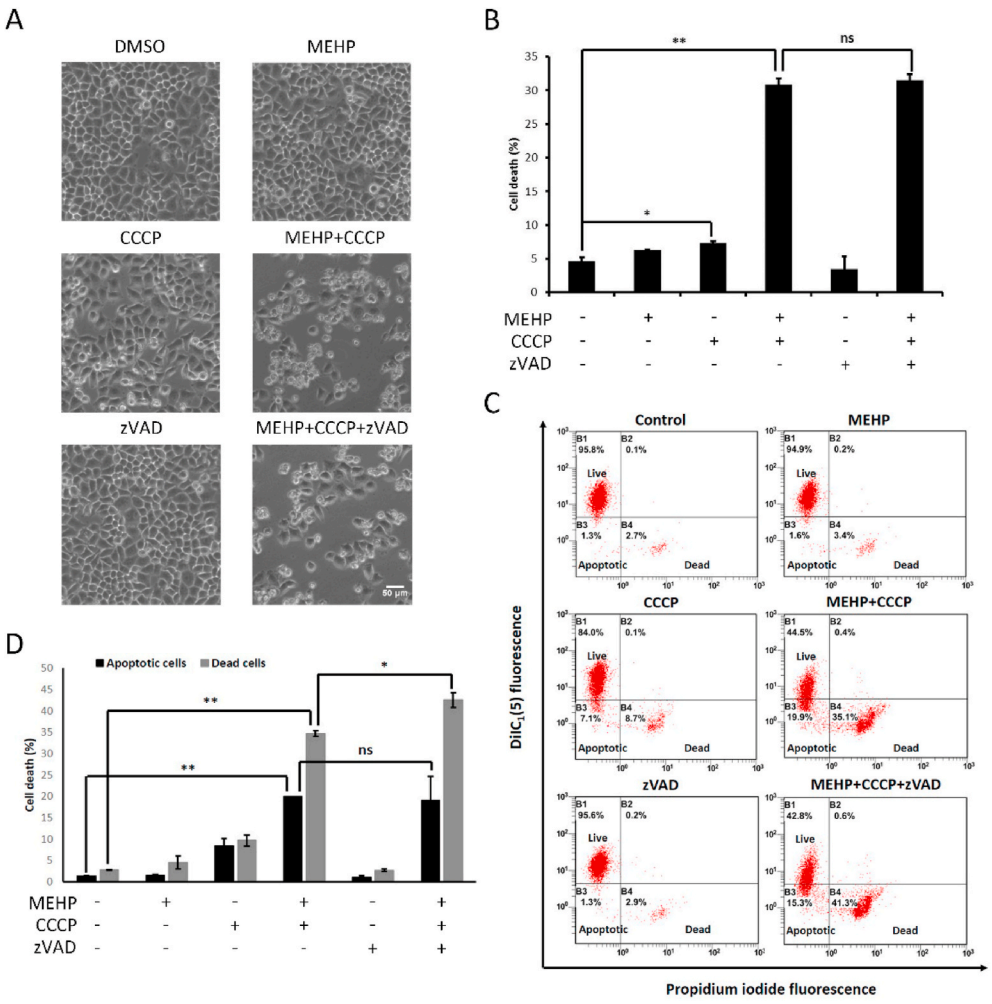

Fig. 5. Mitophagy promotes MEHP-CCCP-induced cell death. (A) HeLa-YFP-Parkin cells were either exposed to MEHP (200 μM) and CCCP (5 μM) respectively or in combination in presence or absence of zVAD (20 μM) for 24 h. Cell morphology was observed under a microscope. Scale bar, 50 μm. **(B)** Cells were treated as in (A), cell pellets were subsequently collected and cell death was quantified using propidium iodide (PI, 5 μg/mL) live exclusion staining coupled with flow cytometry. Statistical significance (*, $P < 0.05$; **, $P < 0.01$; ns, $P > 0.05$; Student's *t*-test) of three independent experiments was indicated in the bar chart. **(C)** After treated as in (A), cells were collected and stained by $DiIC_1(5)$ (50 nM) and PI (1 μg/mL). Flow cytometry was applied to detect the fluorescence intensity of different wavelength lasers. Shown were representative dot-plots of flow cytometry data. **(D)** Quantification of the cell death data from panel C (including apoptotic and dead cells) was shown. Data were presented as means ± SD of three independent experiments (*, $P < 0.05$; **, $P < 0.01$; ns, $P > 0.05$; Student's *t*-test). **(E)** HeLa-YFP-Parkin cells were transfected with a non-targeting siRNA or PINK1 siRNA for 24 h and then co-treated with MEHP (200 μM) and CCCP (5 μM) for another 24 h. Cell morphology was examined by an inverted microscope. Scale bar, 50 μm. **(F)** Cells were treated as in (E) and PI live exclusion assay combined with flow cytometry was performed to analyze the percentage of cell death. Shown were the representative dot-plots of flow cytometry data. **(G)** Data from panel F were presented as means ± SD of three independent experiments (*, $P < 0.05$; Student's *t*-test). **(H)** HeLa-YFP-Parkin cells were either incubated with MEHP (200 μM) and CCCP (5 μM) respectively or in combination with or without of BafA1 (25 nM) for 24 h. Cell morphology was observed under a microscope. Scale bar, 50 μm. **(I)** PI live cell exclusion assay was used to detect the cell death percentage of panel H and shown were the representative dot-plots. **(J)** Percentages of cell death were statistically analyzed and means ± SD were presented (**, $P < 0.01$, Student's *t*-test). MEHP-CCCP-induced mitophagy and cytotoxicity are mediated by ROS. (For interpretation of the references to colour in this figure legend, the reader is referred to the Web version of this article.)

Parkin-mediated mitophagy has been extensively explored [14,15,17]. To further reveal the molecular mechanisms through which MEHP-CCCP regulates mitophagy, we then detected the stabilization of full-length PINK1, accumulation of pSer 65-Ub, mitochondrial translocation and activation of Parkin (Figs. 3 and 4). Similar results were not observed in normal HeLa cells without Parkin expression or after PINK1 knockdown (Figs. 2 and 4), further confirming the critical role of PINK1-Parkin-dependent pathway in this process.

Moreover, we found that MEHP-CCCP induced significant cytotoxicity, which could not be reversed by zVAD (Fig. 5A and B), suggesting that other death mechanisms were involved. Our flow cytometry results confirmed that MEHP-CCCP only induced a small proportion of apoptosis (Fig. 5C and D). At present, the role of mitophagy in cell death remains controversial. Mitophagy is generally believed to be a pro-survival mechanism that helps cells recover from intracellular pressure caused by toxicants. However, some studies also suggest that mitophagy has a pro-death function. For instance, abnormal or excessive mitophagy, which cannot be balanced by adequate biogenesis of newly formed mitochondria, will lead to cell death [21–23]. Indeed, we also found that MEHP-CCCP-induced cytotoxicity was dramatically reduced after PINK1 knockdown (Fig. 5E–G), indicating that mitophagy promoted cell death under our experimental conditions. In addition, the lysosome inhibitor BafA1 inhibited MEHP-CCCP-induced cell death, further supporting the above conclusion (Fig. 5H–J). Xiao et al. reported that pro-oxidants such

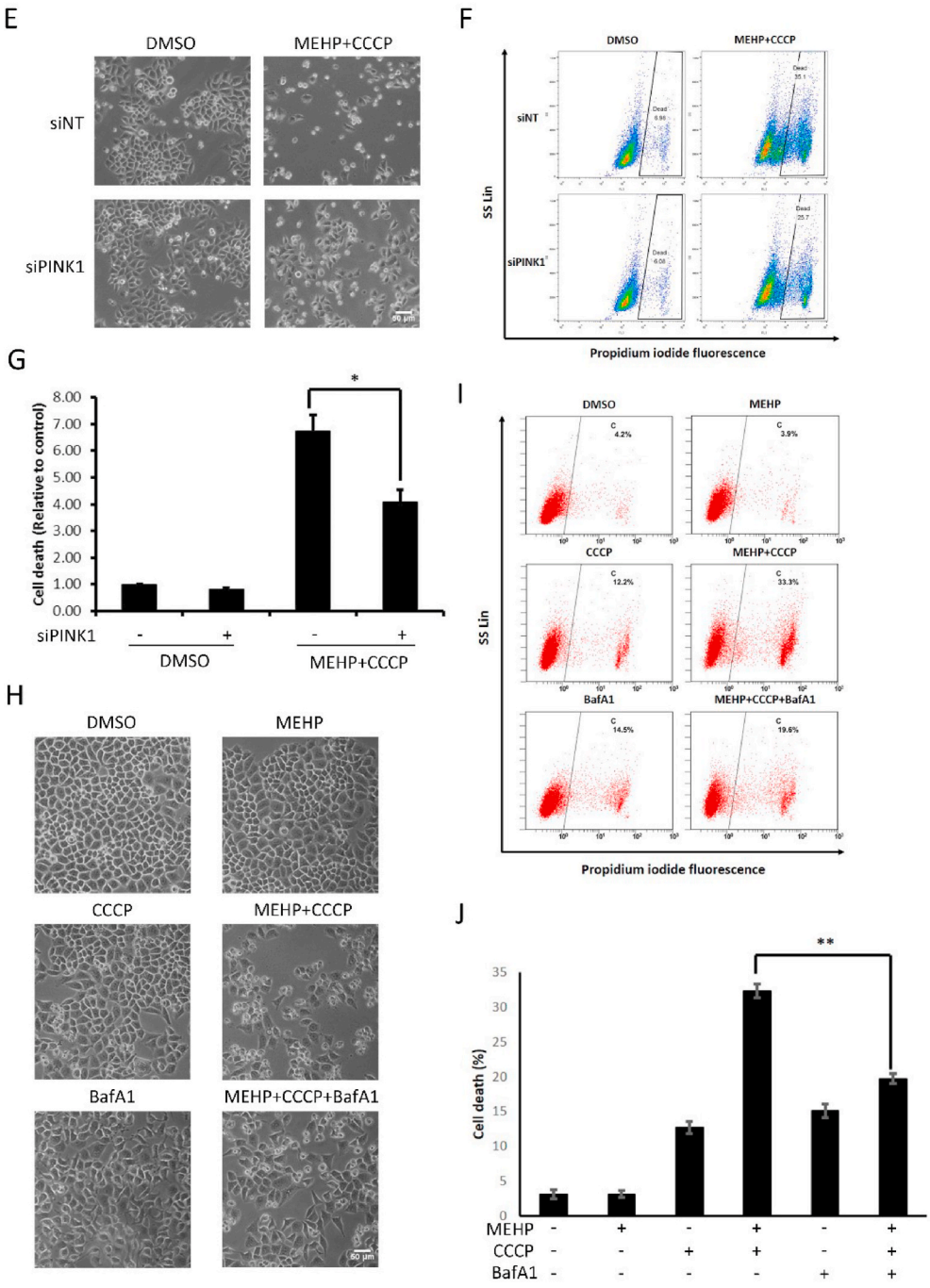

Fig. 5. (*continued*).

as H_2O_2 promoted CCCP-induced Parkin translocation and mitophagy, but pro-oxidants treatment alone did not induce mitophagy [20]. Consistently, our results demonstrated that MEHP was likely to be a pro-oxidant as well, and that ROS mediated MEHP-CCCP-induced Parkin translocation and mitophagy (Fig. 6).

In our study, MEHP (200 μM) exposure alone is not sufficient to induce mitochondrial damage, but the cytotoxicity is greatly enhanced when combined with low-dose CCCP, suggesting that MEHP exposure adds insult to injury when mitochondria have already been damaged. It is reasonable that combined exposure of MEHP and other toxicants in the environment would have similar effects. Thus, understanding joint toxic effects of toxicants is becoming a burning issue for future toxicological research.

In summary, our findings report for the first time the effect of MEHP on mitophagy and its underlying mechanisms, in which mitochondrial ROS play a crucial role, and that mitophagy promotes the cytotoxic effect of MEHP. This study provides a better understanding of the toxic mechanism of EDCs. Since defective mitophagy is implicated in various human diseases such as neurodegenerative disorders, in particular Parkinson's disease, we may also provide some important clues for adverse effects of EDCs on such diseases, promoting rational use of these compounds.

Author contributions

Dajing Xia, Yihua Wu, Han-Ming Shen and Jian Xu designed the study. Jian Xu, Liming Wang, Lihuan Zhang, Fang Zheng, Fang Wang, Jianhang Leng and Keyi Wang performed the experiments for this work.

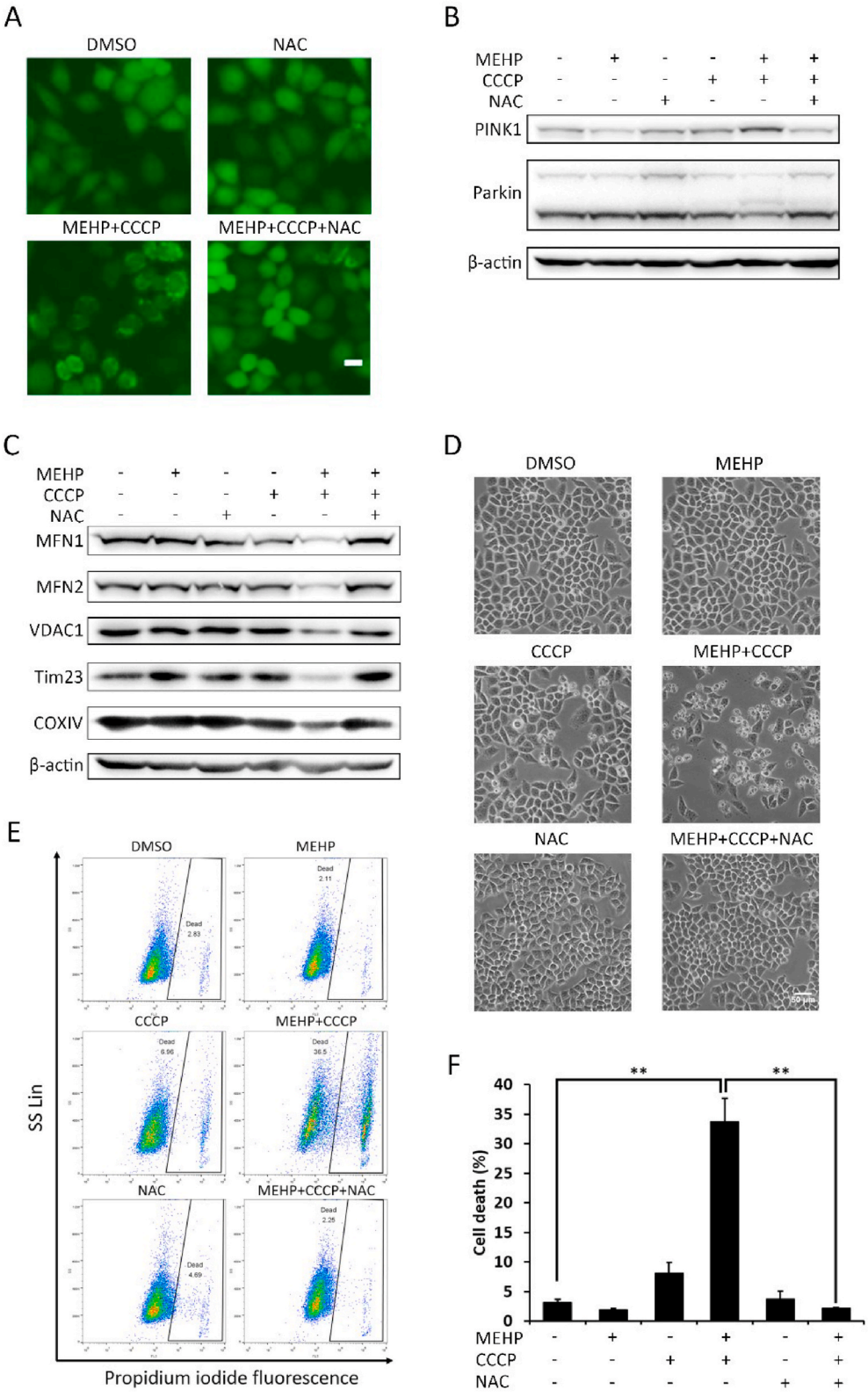

Fig. 6. ROS mediate MEHP-CCCP-induced mitophagy and cytotoxicity. (A) HeLa-YFP-Parkin cells were firstly exposed to MEHP (200 μM) for 24 h and then exposed to CCCP (2.5 μM) for 2 h. NAC (5 mM) was added at the same time of MEHP exposure. YFP-Parkin localization was examined and photographed with a fluorescence microscope. Scale bar, 20 μm. **(B)** HeLa cells stably expressing YFP-Parkin were exposed to MEHP (200 μM, 24 h) or CCCP (2.5 μM, 2 h) respectively, or pre-exposed to MEHP (200 μM) for 24 h, followed by CCCP (2.5 μM) for 2 h in the presence or absence of NAC (5 mM). Cell lysate was harvested and subjected to Western blot to detect the protein levels of PINK1 and Parkin. **(C)** HeLa-YFP-Parkin cells were exposed to MEHP (200 μM, 24 h) or CCCP (2.5 μM, 8 h) respectively, or pre-exposed to MEHP (200 μM) for 24 h, followed by CCCP (2.5 μM) for 8 h in the presence or absence of NAC (5 mM). The degradation of mitochondrial proteins was evaluated by Western blot. **(D)** HeLa-YFP-Parkin cells were either exposed to MEHP (200 μM) and CCCP (5 μM) respectively or in combination in presence or absence of NAC (5 mM) for 24 h. Cell morphology was observed under a microscope. Scale bar, 50 μm. **(E)** Cells were treated as in (D). Cell pellets were then harvested and subjected to PI live cell exclusion assay combined with flow cytometry to detect the cell viability. Shown were the representative dot-plots. **(F)** Statistical analysis of three independent experiments as in (E) was presented as means ± SD (**, $P < 0.01$; Student's *t*-test). (For interpretation of the references to colour in this figure legend, the reader is referred to the Web version of this article.)

Jian Xu and Liming Wang analyzed data in this study. Jian Xu, Liming Wang and Paul Héroux wrote the manuscript. All authors contributed to discussion of the study and revision of this manuscript.

Declaration of competing interest

No potential conflicts of interest were disclosed.

Acknowledgments

We would like to thank Dr. Richard Youle for kindly providing HeLa cells stably expressing YFP-Parkin. This study was supported by the National Natural Science Foundation of China (Grant No: 81773016, 21976155, 31471297), Zhejiang Provincial Natural Science Foundation of China (Grant No: LY18C060001, LY18H160062), Medical Health Science and Technology Project of Hangzhou Municipal Health Commission (A20200097), and Zhejiang University Cancer Center. Thanks for the technical support by the Core Facilities, Zhejiang University School of Medicine.

Appendix A. Supplementary data

Supplementary data to this article can be found online at https://doi.org/10.1016/j.redox.2020.101776.

References

[1] A.C. Gore, V.A. Chappell, S.E. Fenton, J.A. Flaws, A. Nadal, G.S. Prins, J. Toppari, R.T. Zoeller, Executive summary to EDC-2: the endocrine society's second scientific statement on endocrine-disrupting chemicals, Endocr. Rev. 36 (2015) 593–602.
[2] C.W. Tubbs, C.E. McDonough, Reproductive impacts of endocrine-disrupting chemicals on wildlife species: implications for conservation of endangered species, Annual review of animal biosciences 6 (2018) 287–304.
[3] J.A. Rogers, L. Metz, V.W. Yong, Review: endocrine disrupting chemicals and immune responses: a focus on bisphenol-A and its potential mechanisms, Mol. Immunol. 53 (2013) 421–430.
[4] R. Guyot, F. Chatonnet, B. Gillet, S. Hughes, F. Flamant, Toxicogenomic analysis of the ability of brominated flame retardants TBBPA and BDE-209 to disrupt thyroid hormone signaling in neural cells, Toxicology 325 (2014) 125–132.
[5] E.R. Kabir, M.S. Rahman, I. Rahman, A review on endocrine disruptors and their possible impacts on human health, Environ. Toxicol. Pharmacol. 40 (2015) 241–258.
[6] I. Nhanes, Fourth National Report on Human Exposure to Environmental Chemicals, Department of Health and Human Services Centers for Disease Control and Prevention, Atlanta, Georgia, 2009.
[7] D. Gao, Z. Li, H. Wang, H. Liang, An overview of phthalate acid ester pollution in China over the last decade: environmental occurrence and human exposure, Sci. Total Environ. 645 (2018) 1400–1409.
[8] S.S.S. Rowdhwal, J. Chen, Toxic effects of di-2-ethylhexyl phthalate: an overview, BioMed Res. Int. 2018 (2018), 1750368.
[9] S.H. Kim, M.J. Park, Phthalate exposure and childhood obesity, Annals of pediatric endocrinology & metabolism 19 (2014) 69–75.
[10] N. Mizushima, A brief history of autophagy from cell biology to physiology and disease, Nat. Cell Biol. 20 (2018) 521–527.
[11] H. Nakatogawa, K. Suzuki, Y. Kamada, Y. Ohsumi, Dynamics and diversity in autophagy mechanisms: lessons from yeast, Nat. Rev. Mol. Cell Biol. 10 (2009) 458–467.
[12] J. Xu, Y. Wu, G. Lu, S. Xie, Z. Ma, Z. Chen, H.-M. Shen, D. Xia, Importance of ROS-mediated autophagy in determining apoptotic cell death induced by physapubescin B, Redox Biol 12 (2017) 198–207.
[13] A. Abdrakhmanov, V. Gogvadze, B. Zhivotovsky, To eat or to die: deciphering selective forms of autophagy, Trends Biochem. Sci. 45 (2020) 347–364. S0968-0004(0919)30235-X.
[14] J.W. Harper, A. Ordureau, J.M. Heo, Building and decoding ubiquitin chains for mitophagy, Nat. Rev. Mol. Cell Biol. 19 (2018) 93–108.
[15] S. Pickles, P. Vigie, R.J. Youle, Mitophagy and quality control mechanisms in mitochondrial maintenance, Curr. Biol. 28 (2018) R170–R185.
[16] L. Wang, Y.L. Cho, Y. Tang, J. Wang, J.E. Park, Y. Wu, C. Wang, Y. Tong, R. Chawla, J. Zhang, et al., PTEN-L is a novel protein phosphatase for ubiquitin dephosphorylation to inhibit PINK1-Parkin-mediated mitophagy, Cell Res. 28 (2018) 787–802.
[17] L. Wang, H. Qi, Y. Tang, H.-M. Shen, Post-translational modifications of key machinery in the control of mitophagy, Trends Biochem. Sci. 45 (2020) 58–75.
[18] D.A. Kubli, A.B. Gustafsson, Mitochondria and mitophagy: the yin and yang of cell death control, Circ. Res. 111 (2012) 1208–1221.
[19] A.P. Joselin, S.J. Hewitt, S.M. Callaghan, R.H. Kim, Y.H. Chung, T.W. Mak, J. Shen, R.S. Slack, D.S. Park, ROS-dependent regulation of Parkin and DJ-1 localization during oxidative stress in neurons, Hum. Mol. Genet. 21 (2012) 4888–4903.
[20] B. Xiao, X. Deng, G.G.Y. Lim, S. Xie, Z.D. Zhou, K.L. Lim, E.K. Tan, Superoxide drives progression of Parkin/PINK1-dependent mitophagy following translocation of Parkin to mitochondria, Cell Death Dis. 8 (2017) e3097.
[21] H. Abeliovich, Mitophagy: the life-or-death dichotomy includes yeast, Autophagy 3 (2007) 275–277.
[22] V. Corsetti, F. Florenzano, A. Atlante, A. Bobba, M.T. Ciotti, F. Natale, F. Della Valle, A. Borreca, A. Manca, G. Meli, et al., NH2-truncated human tau induces deregulated mitophagy in neurons by aberrant recruitment of Parkin and UCHL-1: implications in Alzheimer's disease, Hum. Mol. Genet. 24 (2015) 3058–3081.
[23] M. Sharma, U.N.R. Jarquín, O. Rivera, M. Kazantzis, M. Eshraghi, N. Shahani, V. Sharma, R. Tapia, S. Subramaniam, Rhes, a striatal-enriched protein, promotes mitophagy via Nix, Proc. Natl. Acad. Sci. U.S.A. 116 (2019) 23760–23771.
[24] X. Chen, J. Wang, Q. Qin, Y. Jiang, G. Yang, K. Rao, Q. Wang, W. Xiong, J. Yuan, Mono-2-ethylhexyl phthalate induced loss of mitochondrial membrane potential and activation of Caspase 3 in HepG2 cells, Environ. Toxicol. Pharmacol. 33 (2012) 421–430.
[25] X. Wu, L. Jiang, X. Sun, X. Yao, Y. Bai, X. Liu, N. Liu, X. Zhai, S. Wang, G. Yang, Mono(2-ethylhexyl) phthalate induces autophagy-dependent apoptosis through lysosomal-mitochondrial axis in human endothelial cells, Food Chem. Toxicol. 106 (2017) 273–282.
[26] I. Savchuk, O. Soder, K. Svechnikov, Mono-2-ethylhexyl phthalate stimulates androgen production but suppresses mitochondrial function in mouse leydig cells with different steroidogenic potential, Toxicol. Sci. : an official journal of the Society of Toxicology 145 (2015) 149–156.
[27] G. Fu, J. Dai, D. Zhang, L. Zhu, X. Tang, L. Zhang, T. Zhou, P. Duan, C. Quan, Z. Zhang, et al., Di(2-ethylhexyl) phthalate induces apoptosis through mitochondrial pathway in GC-2 spd cells, Environ. Toxicol. 32 (2017) 1055–1064.
[28] G. Yang, W. Zhang, Q. Qin, J. Wang, H. Zheng, W. Xiong, J. Yuan, Mono(2-ethylhexyl) phthalate induces apoptosis in p53-silenced L02 cells via activation of both mitochondrial and death receptor pathways, Environ. Toxicol. 30 (2015) 1178–1191.
[29] W. Wang, F. Zhang, L. Li, F. Tang, S.L. Siedlak, H. Fujioka, Y. Liu, B. Su, Y. Pi, X. Wang, MFN2 couples glutamate excitotoxicity and mitochondrial dysfunction in motor neurons, J. Biol. Chem. 290 (2015) 168–182.
[30] T.B. Fonseca, A. Sanchez-Guerrero, I. Milosevic, N. Raimundo, Mitochondrial fission requires DRP1 but not dynamins, Nature 570 (2019) E34–e42.
[31] A.B. Knott, G. Perkins, R. Schwarzenbacher, E. Bossy-Wetzel, Mitochondrial fragmentation in neurodegeneration, Nat. Rev. Neurosci. 9 (2008) 505–518.
[32] C.R. Chang, C. Blackstone, Cyclic AMP-dependent protein kinase phosphorylation of Drp1 regulates its GTPase activity and mitochondrial morphology, J. Biol. Chem. 282 (2007) 21583–21587.
[33] S. Xu, P. Wang, H. Zhang, G. Gong, N. Gutierrez Cortes, W. Zhu, Y. Yoon, R. Tian, W. Wang, CaMKII induces permeability transition through Drp1 phosphorylation during chronic beta-AR stimulation, Nat. Commun. 7 (2016), 13189.
[34] L.A. Kane, M. Lazarou, A.I. Fogel, Y. Li, K. Yamano, S.A. Sarraf, S. Banerjee, R. J. Youle, PINK1 phosphorylates ubiquitin to activate Parkin E3 ubiquitin ligase activity, J. Cell Biol. 205 (2014) 143–153.
[35] A. Kazlauskaite, C. Kondapalli, R. Gourlay, D.G. Campbell, M.S. Ritorto, K. Hofmann, D.R. Alessi, A. Knebel, M. Trost, M.M. Muqit, Parkin is activated by PINK1-dependent phosphorylation of ubiquitin at Ser65, Biochem. J. 460 (2014) 127–139.
[36] F. Koyano, K. Okatsu, H. Kosako, Y. Tamura, E. Go, M. Kimura, Y. Kimura, H. Tsuchiya, H. Yoshihara, T. Hirokawa, et al., Ubiquitin is phosphorylated by PINK1 to activate parkin, Nature 510 (2014) 162–166.
[37] K. Shiba-Fukushima, T. Arano, G. Matsumoto, T. Inoshita, S. Yoshida, Y. Ishihama, K.Y. Ryu, N. Nukina, N. Hattori, Y. Imai, Phosphorylation of mitochondrial polyubiquitin by PINK1 promotes Parkin mitochondrial tethering, PLoS Genet. 10 (2014), e1004861.
[38] C. Kondapalli, A. Kazlauskaite, N. Zhang, H.I. Woodroof, D.G. Campbell, R. Gourlay, L. Burchell, H. Walden, T.J. Macartney, M. Deak, et al., PINK1 is activated by mitochondrial membrane potential depolarization and stimulates Parkin E3 ligase activity by phosphorylating Serine 65, Open Biol 2 (2012), 120080.
[39] K. Shiba-Fukushima, Y. Imai, S. Yoshida, Y. Ishihama, T. Kanao, S. Sato, N. Hattori, PINK1-mediated phosphorylation of the Parkin ubiquitin-like domain primes mitochondrial translocation of Parkin and regulates mitophagy, Sci. Rep. 2 (2012) 1002.
[40] Z. Fu, F. Zhao, K. Chen, J. Xu, P. Li, D. Xia, Y. Wu, Association between urinary phthalate metabolites and risk of breast cancer and uterine leiomyoma, Reprod. Toxicol. 74 (2017) 134–142.
[41] N. Liu, L. Jiang, X. Sun, X. Yao, X. Zhai, X. Liu, X. Wu, Y. Bai, S. Wang, G. Yang, Mono-(2-ethylhexyl) phthalate induced ROS-dependent autophagic cell death in human vascular endothelial cells, Toxicol. Vitro : an international journal published in association with BIBRA 44 (2017) 49–56.